

TiB₂ PARTICLE DETECTION IN LIQUID ALUMINUM VIA LASER INDUCED BREAKDOWN SPECTROSCOPY

S. W. Hudson¹, J. Craparo², R. De Saro², D. Apelian¹

¹ Worcester Polytechnic Institute; 100 Institute Road, Worcester, MA, 01609, USA

² Energy Research Company, 1250 South Avenue, Plainfield, NJ, 07062, USA

Keywords: Metal Cleanliness, LIBS, Inclusions, Liquid Aluminum

Abstract

Because aluminum alloy castings are becoming commonplace for critical applications in the automotive and aerospace industries, tight control over the cleanliness of the melt (mitigation of solid particle inclusions) and microstructure must be achieved. In order to control cleanliness, it must first be well defined and measured. Very few techniques exist in industry that can quantitatively measure inclusion levels in-situ. Laser-induced breakdown spectroscopy (LIBS) is presented as a promising technique to quantify solid particles, desired or undesired, in aluminum melts. By performing LIBS with subsequent statistical analysis on liquid Al with varying amounts of TiB₂ particles, calibration curves for B and Ti were generated.

Introduction

There is a plethora of laboratory and foundry floor techniques to assess inclusion content in aluminum and its alloys. They include methods ranging from traditional optical metallography to filtration and ultrasound with each method having its own pros and cons [1-6]. Other than LiMCA (Liquid Metal Cleanliness Analyzer), a coulter counter technique, and Metalvision, an ultrasonic technique, there are no other methods of measuring inclusion concentration in-situ [7]. One of the main drawbacks to these techniques is their inability to discern particles with different chemistries.

Laser-induced breakdown spectroscopy (LIBS) has been of great interest to the metals processing field as tool for bulk chemistry measurement. Similar to conventional OES, LIBS uses a short laser pulse to form a micro-plasma from a sample of metal. The plasma light is processed with a spectrograph to determine the concentration of elements present. The volume ablated in this process is quite small (10^{-8} to 10^{-5} cm³ depending on laser parameters and substrate material) and allows for many measurements to be taken without compromising the bulk material [8]. LIBS requires a direct line of sight to the substrate for analysis, making it attractive for use in extreme environments. LIBS systems have been adapted for high temperature applications and have been used to measure composition of molten metals [9]. The fundamentals of LIBS can be found in several books and review papers [10-12].

In this work, the premise has been that LIBS can be used as a means of detecting inclusions and second phase particles in molten metals. If a particle is present in the sampling volume, the spectra will reveal its presence and chemistry. Such work has been performed on solid steel [13, 14] and aluminum [15, 16]. Studies with Al₂O₃, AlB₂, and SiC particles in liquid Al have been recently performed by the authors [16-18].

Experimental

Sample Preparation

99.99% pure aluminum (Belmont Metals) was melted in an electric resistance furnace to a temperature of 800±1°C. Al-Ti-B master alloy rods (Milward Alloys) were used to introduce boride particles into the melt. Base metal and rod additions were weighed beforehand to ensure each charge had a total weight of 2.5 kg. The melt was gently agitated immediately after master alloy addition. Composition of the base aluminum is compiled in Table I. Weights and compositions of each trial are compiled in Table II.

Elemental composition of the metal was measured by Spark OES (SpectroMaxX). The maximum level of boron detectable via OES was 0.026 wt.%. To estimate the actual amount of boron in the metal, the measured amount of Ti was multiplied by the B/Ti ratio of the master alloy.

Table I: Composition of base aluminum used in experiments

Element	Si	Fe	Ga	Others	Al
wt.%	0.00079	0.00092	0.0007	Trace	99.995

Table II: Weights, compositions, and elemental ratio of each experiment.

Base Al (kg)	Master Alloy (kg)	Ti/B Ratio	Composition (wt.%, From OES)	
			Ti	B
2.40	Al-3Ti-1B (0.10)	3	0.092	0.030
2.30	Al-3Ti-1B (0.20)	3	0.151	0.050
2.22	Al-3Ti-1B (0.30)	3	0.319	0.162
2.37	Al-2.6Ti-2.2B (0.10)	1.18	0.064	0.054
2.38	Al-5Ti-1B (0.10)	5	0.205	0.041

LIBS Measurements

LIBS trials were performed using a ceramic probe developed by Energy Research Company (Plainfield, NJ) [19]. The probe was submerged 5-7cm below the melt surface. Purified nitrogen gas from a liquid source was used for coolant and bubbling flow. The immersed probe is shown in Figure 1.

The laser apparatus consisted of a Q-switched, 20 Hz Nd:YAG laser, operated at 1064 nm with a 50 mJ pulse energy (Quantel Laser). Emitted plasma light was collected via a fiber-optic cable and fed into an Echelle-type spectrometer (LLA Instruments).

10-20 test measurements were taken to account for any transient signals. 500 successive laser shots were then fired one at a time

into the melt. Spectra data was gathered with ESAWIN software and analyzed via Microsoft Excel. Measurement frequency was approximately 1 Hz.



Figure 1: LIBS Probe Immersed in the furnace [16].

A small amount of metal was also drawn from the crucible and cast in an iron, cylindrical mold. Cast cylinders had a 7.5 cm height and 4 cm diameter. The bottom 1.5 cm of each cylinder was then sectioned off for metallographic analysis.

Microanalysis

Samples were mounted in diallyl phthalate studs, ground, and polished with diamond suspension on a semi-automatic polisher. Back-scatter SEM/EDS analysis was employed to determine particle composition. ASPEx analysis software was used to determine diameter, volume fraction, of the inclusions. Particles were identified based on contrast and EDS count. Particles with both bright contrast (high video level) and high Ti content (> 3% after subtracting background Al signal) were classified as TiB₂.

Results and Discussion

LIBS Measurements

Boron's highest intensity peaks in emission spectroscopy occur within the 200-300 nm range. Boron's emission line at 249.772 nm was analyzed for these experiments. Titanium produces a large number of lines within the 300-400 nm range. Its peak at 399.8636 nm was used to analyze the effect of Ti concentration on the melt. To analyze individual particles, a weaker but more sensitive peak at 323.4513 nm was used. To account for the variability in signal between individual measurements, boron and titanium peak intensities were normalized by the intensity of the aluminum peak at 308.852 nm [20].

As seen in Figure 2 and 3, elemental signal noticeably increases with solute content. Data points represent the averaged signal over 500 laser pulses. There is a good linear agreement for the ranges

of Ti and B desired in grain refinement. Depending on the alloy, typical target chemistries range from 0.2-0.5 wt.% Ti and 0.01-0.03 wt.% B [21]. The solubility of boron in liquid aluminum is extremely low (less than 0.05% at 750-800°C) [22]. This is lower than the typical limits of detection of LIBS for solute elements in aluminum [23]. Therefore, the assumption can be made that any time a boron line is detected, a boron containing particle was present in the sampling volume.

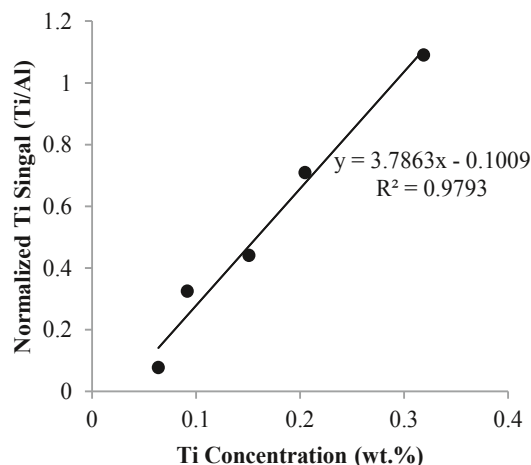


Figure 2: Calibration curve of average Ti signal vs. concentration.

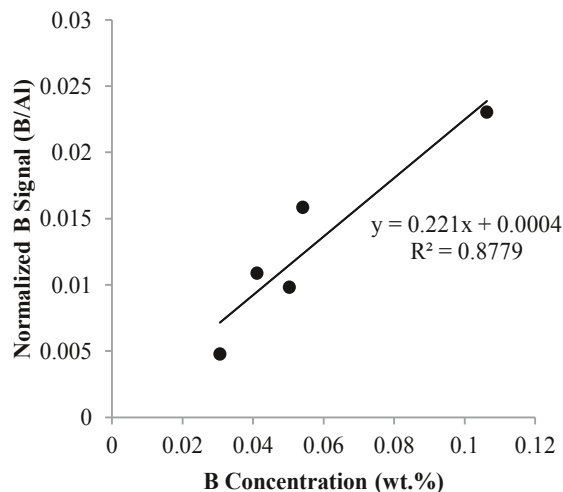


Figure 3: Calibration curve of average B signal vs. concentration.

Two-tailed analysis of variance (ANOVA) was applied to the LIBS datasets. Statistics on each element, compiled in Table III, show that with 95% confidence there is no statistically significant overlap between the data.

Table III: ANOVA on Ti and B measurements

Element	Calculated F	p-Value	Critical F
B	33.268	4.52×10^{-27}	2.375
Ti	286.417	7.40×10^{-203}	2.375

The Nalimov test was used to separate baseline signal from that of a particle hit. For boron, the solubility is extremely low in liquid aluminum and below the sensing capabilities of the spectrometer. Therefore, any substantial signal above the background can be attributed to a boride particle. For titanium, there is an appreciable amount dissolved within the matrix. In this case, the baseline is the signal coming from dissolved titanium. By using the Nalimov test on the Ti and B datasets, it was found that for approximately 10% of the time, a spike in B intensity did not coincide with a spike in Ti intensity. This indicates that the test requires some optimization, or perhaps a more conditional analysis approach is required to separate out background elemental signal from signal corresponding to a particle hit. Application of the Nalimov test to Ti and B signals yielded linear relationships between average particle hit intensities and volume fraction determined by microanalysis (Figure 4 and 5). Even though there is a linear relationship between particle hit intensity and volume fraction, using overall Ti and B signal from Figure 2 and 3 can be used to determine when grain refining elements are at their optimal levels.

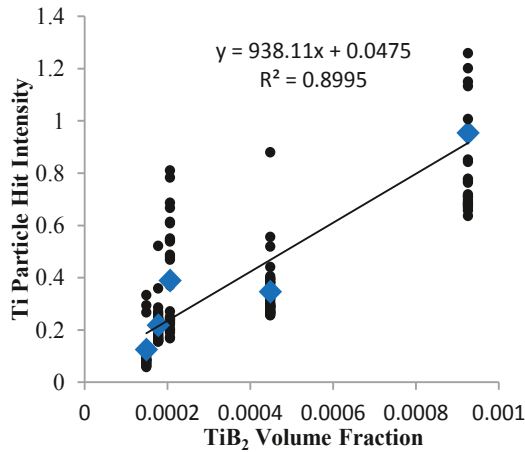


Figure 4: Ti particle hits from LIBS as a function of TiB₂ volume fraction. Diamonds correspond to average values.

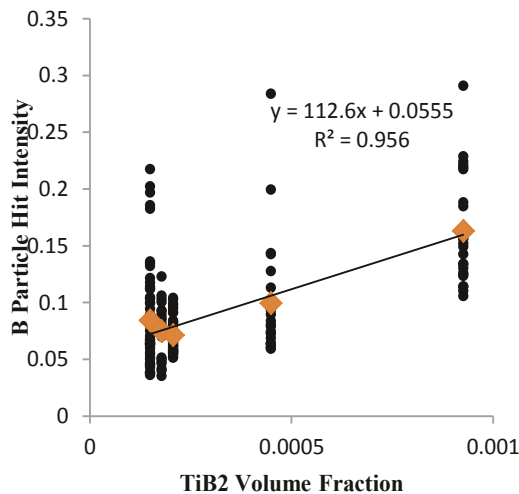


Figure 5: B particle hits from LIBS as a function of TiB₂ volume fraction. Diamonds correspond to average values.

Microanalysis

Irrespective of volume fraction, most TiB₂ particles were less than 20 μm and were narrowly distributed. Little to no AlB₂ or TiAl₃ particles were observed during microanalysis. TiB₂ was seen as bright particles in the pure Al matrix. Irrespective of volume fraction, over 90% of particles were less than 10 μm and were narrowly distributed (Figure 6). It should be noted that LiMCA, with a detection limit of 20 μm, would in principle be unable to detect such particles. The fact that they were able to be detected by LIBS is significant.

Both the number and volume fraction of TiB₂ particles are linearly proportional to the concentration of Ti and B. However, deviations occurred when the ratio of Ti/B was too skewed. It is known that, for most alloys, the optimal ratio is approximately 2.22 wt.% Ti to 1 wt.% B for optimal grain refinement [21]. If the ratio is too high, the resultant volume fraction of particles will decrease due to the lack of boron in the matrix. This can be seen in Figure 7, where the data point for Al-0.205Ti-0.041B (Ti/B ratio of 5) significantly deviates from the linear relationship.

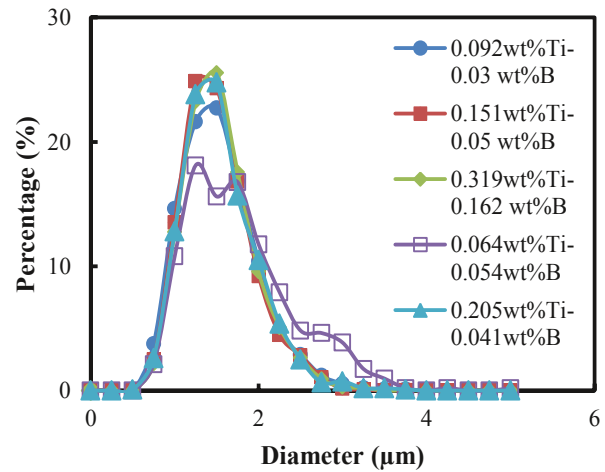


Figure 6: TiB₂ particle size distribution.

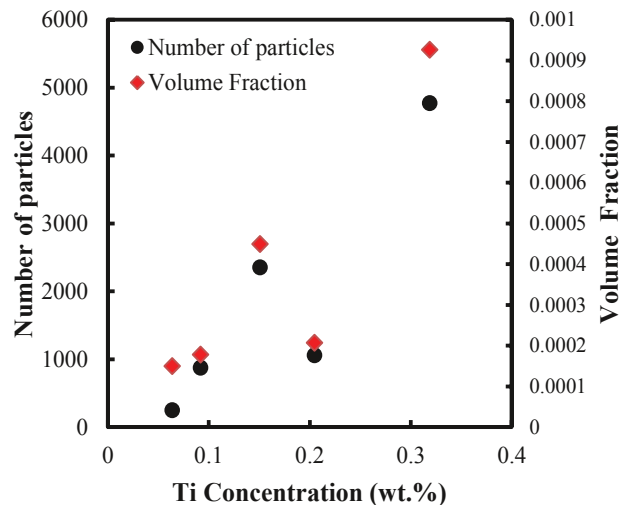


Figure 7: TiB₂ particle count and volume fraction as a function of Ti concentration.

Conclusions and Future Work

Pure aluminum with varying amounts of Al-Ti-B master alloys were analyzed using in-situ LIBS. It was found that over the course of many laser measurements, TiB₂ particles could be detected by monitoring Ti and B signal. Calibration curves were developed for Ti and B in pure Al within the compositional ranges for grain refinement, allowing LIBS to be used as a possible tool for monitoring grain refining elements. Nearly all particles that were observed in microanalysis were less than 6 μm in size, well below the 20 μm sensing limit of LiMCA. The Nalimov test was used to determine elemental signal that was not from the bulk chemistry, but from particles. In the case of separating out Ti signal from a particle hit from that in the bulk metal, the Nalimov test performs a reasonable job. However, its identification of false negative requires a more conditional analysis.

Due to the small size of the melt, there was enough turbulence to enable random sampling with the laser. However, this is not always the case in larger melts. Further tests with larger melt sizes need to be conducted.

Acknowledgements

We kindly thank Dave Smith and Wenwu Shi (Foseco) for metallography and image analysis as well as the member consortium of WPI's Advanced Casting Research Center for funding this ongoing project.

References

1. S. Poynton, M. Brandt, and J. Grandfield, "A Review of Inclusion Detection Methods in Molten Aluminium," (Paper Presented at Light Metals 2009, 138th TMS Annual Meeting, San Francisco, CA, 15-19 February 2009), 681-687.
2. J. Wannasin, D. Schwam, and J.F. Wallace, "Evaluation of Methods for Metal Cleanliness Assessment in Die Casting," *Journal of Materials Processing Technology*, 191 (3) (2007), 242-246.
3. T.A. Utigard and I.D. Sommerville, "Cleanliness of Aluminum and Steel: A Comparison of Assessment Methods," (Paper Presented at Light Metals 2005, 134th TMS Annual Meeting, San Francisco, California, 13-17 February 2005), 951-956.t
4. O. Lashkari et al., "X-Ray Microtomographic Characterization of Porosity in Aluminum Alloy A356," *Metallurgical and Materials Transactions A*, 40 (4) (2009), 991-999.
5. D. Neff, "Using Filters and Evaluating Their Effectiveness in High Pressure Diecasting," (Paper presented at NADCA Congress, Chicago, IL, September 2002).
6. D. Apelian, "How clean is the metal you cast? The issue of assessment; a status report," (Paper presented at the 3rd International Conference on Molten Aluminum Processing, Orlando, FL, 9-10 November 1992), 1-15.
7. Grandfield, J., D.G. Eskin, and I.F. Bainbridge, *Melt Refining and Impurity Control*, in *Direct-Chill Casting of Light Alloys: Science and Technology*. 2013, John Wiley & Sons: Hoboken, NJ.
8. W.T.Y. Mohamed, "Improved LIBS Limit of Detection of Be, Mg, Si, Mn, Fe and Cu in Aluminum Alloy Samples Using a Portable Echelle Spectrometer with ICCD Camera," *Optics & Laser Technology*, 40 (1) (2008), 30-38.
9. A.K. Rai, F.Y. Yueh, and J.P. Singh, "Laser-Induced Breakdown Spectroscopy of Molten Aluminum Alloy," *Appl. Opt.*, 42 (12) (2003), 2078-2084.
10. D.W. Hahn and N. Omenetto, "Laser-Induced Breakdown Spectroscopy (LIBS), Part I: Review of Basic Diagnostics and Plasma-Particle Interactions: Still-Challenging Issues Within the Analytical Plasma Community," *Appl Spectrosc.*, 64 (12) (2010), 335A-366A.
11. D.W. Hahn and N. Omenetto, "Laser-Induced Breakdown Spectroscopy (LIBS), Part II: Review of Instrumental and Methodological Approaches to Material Analysis and Applications to Different Fields," *Appl Spectrosc.*, 66 (4) (2012), 347-419.
12. L. Radziemski and D. Cremers, "A Brief History of Laser-Induced Breakdown Spectroscopy: From the Concept of Atoms to LIBS 2012," *Spectrochimica Acta Part B: Atomic Spectroscopy*, 87 (2013), 3-10.
13. H.M. Kuss, H. Mittelstaedt, and G. Mueller, "Inclusion Mapping and Estimation of Inclusion Contents in Ferrous Materials by Fast Scanning Laser-Induced Optical Emission Spectrometry," *Journal of Analytical Atomic Spectrometry*, 20 (2005), 730-735.
14. H. Falk and P. Wintjens, "Statistical Evaluation of Single Sparks," *Spectrochimica Acta Part B-Atomic Spectroscopy*, 53 (1) (1998), 49-62.
15. I.V. Cravetchi, et al., "Scanning Microanalysis of Al Alloys by Laser-Induced Breakdown Spectroscopy," *Spectrochimica Acta Part B: Atomic Spectroscopy*, 59(9) (2004), 1439-1450.
16. S.W. Hudson and D. Apelian, "Clean Aluminum Processing: New Avenues for Measurement and Analysis," (Paper Presented at Light Metals 2014, 143rd TMS Annual Meeting, San Diego, CA, 16-20 February 2014) 1025-1029.
17. S.W. Hudson and D. Apelian, "Boride Particle Detection in Al Melts Via Laser Induced Breakdown Spectroscopy," (Paper Presented at the Materials Science & Technology 2014, Pittsburgh, PA, 12-16 October 2014), 735-742.
18. S.W. Hudson, et al., "SiC Particle Detection in Liquid Aluminum Via Laser Induced Breakdown Spectroscopy," (Paper Presented at Light Metals 2015, 144th TMS Annual Meeting, Orlando, FL, 15-19 March 2015), 987-990.
19. R. De Saro, A. Weisberg, and J. Craparo. "In Situ, Real Time Measurement of Aluminum Melt Chemistry," (Paper Presented at Light Metals 2003, 132nd TMS Annual Meeting, San Diego, CA, 2-6 March 2003), 1103-1107.
20. Kramida, A., et al., *NIST Atomic Spectra Database*, 2014.
21. R.B. Tuttle., *Foundry engineering: the metallurgy and design of castings*. 2012, United States: CreateSpace.
22. H. Duschanek and P. Rogl, "The Al-B (Aluminum-Boron) System," *Journal of Phase Equilibria*, 15(5) (1994), 543-552.

23. L. Paksy, et al., "Production Control of Metal Alloys by Laser Spectroscopy of the Molten Metals Part 1: Preliminary Investigations," *Spectrochimica Acta. Part B: Atomic Spectroscopy*, 51(2) (1996), 279-290.